Differential effects of lobe A and lobe B of the Conserved Oligomeric Golgi complex on the stability of β1,4-galactosyltransferase 1 and α2,6-sialyltransferase 1

Romain Peanne[2], Dominique Legrand[2], Sandrine Duvet[2], Anne-Marie Mir[2], Gert Matthijs[3], Jack Rohrer[4,5,6], and François Foulquier[1,2,5]

[2]Unité de Glycobiologie Structurale et Fonctionnelle UMR/CNRS 8576, IFR147, Université des Sciences et Technologies de Lille, F-59655 Villeneuve d'Ascq, France; [3]Laboratory for Molecular Diagnosis, Center for Human Genetics, University of Leuven, B-3000 Leuven, Belgium; and [4]Institute of Physiology, University of Zürich, CH-8057 Zürich, Switzerland

Initially described by Jaeken et al. in 1980, congenital disorders of glycosylation (CDG) is a rapidly expanding group of human multisystemic disorders. To date, many CDG patients have been identified with deficiencies in the conserved oligomeric Golgi (COG) complex which is a complex involved in the vesicular intra-Golgi retrograde trafficking. Composed of eight subunits that are organized in two lobes, COG subunit deficiencies have been associated with Golgi glycosylation abnormalities. Analysis of the total serum *N*-glycans of COG-deficient CDG patients demonstrated an overall decrease in terminal sialylation and galactosylation. According to the mutated COG subunits, differences in late Golgi glycosylation were observed and led us to address the question of an independent role and requirement for each of the two lobes of the COG complex in the stability and localization of late terminal Golgi glycosylation enzymes. For this, we used a small-interfering RNAs strategy in HeLa cells stably expressing green fluorescent protein (GFP)-tagged β1,4-galactosyltransferase 1 (B4GALT1) and α2,6-sialyltransferase 1 (ST6GAL1), two major Golgi glycosyltransferases involved in late Golgi *N*-glycosylation. Using fluorescent lectins and flow cytometry analysis, we clearly demonstrated that depletion of both lobes was associated with deficiencies in terminal Golgi N-glycosylation. Lobe A depletion resulted in dramatic changes in the Golgi structure, whereas lobe B depletion severely altered the stability of B4GALT1 and ST6GAL1. Only MG132 was able to rescue their steady-state levels, suggesting that B4GALT1- and ST6GAL1-induced degradation are likely the consequence of an accumulation in the endoplasmic reticulum (ER), followed by a retrotranslocation into the cytosol and proteasomal degradation. All together, our results suggest differential effects of lobe A and lobe B for the localization/stability of B4GALT1 and ST6GAL1. Lobe B would be crucial in preventing these two Golgi glycosyltransferases from inappropriate retrograde trafficking to the ER, whereas lobe A appears to be essential for maintaining the overall Golgi structure.

Introduction

The endoplasmic reticulum (ER) and Golgi apparatus are key organelles in the secretory pathway of proteins and lipids. Among the post-translational modifications occurring in these distinct compartments, one of the most important is the glycosylation consisting in the covalent attachment of glycans to proteins (Van den Steen et al. 1998; Ferrari et al. 2001; Helenius and Aebi 2004). *N*-Glycosylation first takes place in the ER lumen with the assembly of a dolichol-linked oligosaccharide, later transferred from its lipid carrier to nascent proteins. Within the ER but especially in the Golgi apparatus, a complete remodeling of the glycan structure is achieved by the subsequent action of glycosyltransferases and glycosidases resulting in a mature complex type *N*-glycan (Kornfeld R and Kornfeld S 1985). A correct glycan structure, crucial for many cellular biological functions, not only depends on the activity of glycosylation enzymes, but also requires their specific localization within the Golgi cisternae (see Foulquier 2009 for review).

The molecular mechanisms by which this distribution within the different Golgi stacks is established and maintained are still obscure but seem to be based on a dynamic process, achieved by a finely regulated balance between anterograde and retrograde trafficking (Fotso et al. 2005). Different models have been proposed regarding the vesicular Golgi trafficking. For several years, the main models were the vesicular transport and the cisternal maturation models (Pelham and

---

[1]To whom correspondence should be addressed: Tel: +33-320-43-44-30; Fax: +33-320-43-65-55; e-mail: francois.foulquier@univ-lille1.fr
[5]These authors contributed equally to this work.
[6]Present address: Institute of Biotechnology, Zurich University of Applied Sciences, 8820 Wädenswil, Switzerland.

Rothman 2000; Elsner et al. 2003, review). Recently, a third model was however proposed by Patterson et al. (2008). This model postulates that the mammalian Golgi apparatus presents a two-dimensional gradient in lipid composition, governing the steady-state distribution of transmembrane cargo proteins and glycosylation enzymes.

Independent of the specific model, the precise distribution of the glycosyltransferases within the Golgi apparatus requires a complex transport machinery. Part of the machinery consists of the conserved oligomeric Golgi (COG) complex Ungar et al. (2002), a peripheral Golgi octa heteromeric complex composed of eight subunits (Cog1–8) arranged in two distinct lobes: lobe A (Cog1–4) and lobe B (Cog5–8) whose cellular roles have not yet been fully elucidated. Several studies highlighted its functions in trafficking and/or stability of Golgi glycosylation enzymes. Indeed, a set of seven COG sensitive, type II integral membrane proteins called GEARs presented decreased steady-state levels in ldlB and ldlC Chinese hamster ovary (CHO) cell lines, which are deficient in Cog1 and Cog2, respectively (Oka et al. 2004). These proteins have been found to accumulate in "COG complex-dependent" (CCD) vesicles in small-interfering RNA (siRNA)-induced Cog3-depleted cells (Zolov and Lupashin 2005). Further analysis also suggested that the COG complex regulated the efficient vesicle tethering of Golgi enzymes by a constant retrieval to their correct localization in CCD vesicles (Shestakova et al. 2006). The COG complex might act as a tethering factor, mediating an interaction between an ER-derived vesicle and its Golgi target via SNARE-mediated fusion (see Ungar et al. 2006 for review). The critical requirement of COG proteins for Golgi glycosylation has been demonstrated by the identification of several COG-deficient congenital disorders of glycosylation (CDG) patients. Initially described by Jaeken et al. (1980), two types of CDGs were defined according to the cellular localization of the deficiency: type I CDGs caused by alterations in the assembly or transfer of the dolichol-linked oligosaccharide precursor and type II CDGs involving defects in the processing of protein bound N-linked oligosaccharides within the ER and/or Golgi. The first CDG case linked to COG subunit deficiency was documented by Wu et al. (2004). Up to date, patients presenting mutations in Cog1 and Cog4–8 subunits have been identified (Wu et al. 2004; Spaapen et al. 2005; Foulquier et al. 2006; Steet and Kornfeld 2006; Foulquier et al. 2007; Kranz et al. 2007; Ng et al. 2007; Paesold-Burda et al. 2009; Reynders et al. 2009; Lübbehusen et al. 2010). According to the mass spectrometry analysis of total serum, we have shown that both N- and O-glycosylation were impaired in COG-deficient CDG patients (Reynders et al. 2009). Indeed, an overall decrease in both sialylation and galactosylation and strong differences in the relative amounts and the presence of unexpected oligosaccharide structures were observed in all COG-deficient CDG patients tested so far. In fibroblasts derived from patients, mutations of some COG subunits resulted in significantly reduced activities of nucleotide-sugar transporters and a decreased stability of some Golgi enzymes such as Golgi mannosidase II and β1,4-galactosyltransferase 1 (B4GALT1; Foulquier et al. 2006, 2007; Kranz et al. 2007). Depending on the various COG-deficient patient cells, differences mostly

affecting the late Golgi glycosylation were observed. These differences that are likely to result from the severity of the mutation within the given subunits led us to address the question of an independent role and requirement for each of the two lobes of the COG complex in the stability and/or the localization of late terminal Golgi glycosylation enzymes. Given that two main Golgi glycosyltransferases are involved in the late Golgi N-glycosylation reaction: the β1,4-galactosyltransferase 1 (B4GALT1) and the α2,6-sialyltransferase 1 (ST6GAL1), a strategy with siRNAs to knockdown the expression of Cog3p and Cog7p for the lobe A and lobe B, respectively was used in HeLa cells stably expressing either green fluorescent protein (GFP)-tagged B4GALT1 (GalT1-GFP) or GFP-tagged ST6GAL1 (SiaT1-GFP).

We demonstrated that Cog3p depletion, while accompanied by an extensive Golgi fragmentation, had no effects on the steady-state levels of B4GALT1 and ST6GAL1. Strikingly and at the opposite, we could show that Cog7 depletion severely altered the steady-state levels of both enzymes. A quantitative polymerase chain reaction (QPCR) approach allowed us to exclude any transcriptional regulation of B4GALT1 and ST6GAL1 in response to siRNA-mediated disruption of the lobe B of the COG complex. Furthermore, we used different lysosomal and proteasomal inhibitors to assess the stability of both enzymes under siCog7. Interestingly, only treatment with MG132 was able to rescue the steady-state level of both B4GALT1 and ST6GAL1 following Cog7p depletion. Therefore, we concluded that lobe B of the COG complex is crucial for the stability of these two enzymes. Interestingly, both Cog3p and Cog7p depletion were correlated with deficiencies in the terminal N-glycosylation as estimated by flow cytometry analysis with FITC-labeled lectins. Moreover, we showed that the disruption of either lobe A or lobe B of the COG complex can also affect different subsets of secretory-pathway-related proteins. Our data then suggest the existence of functional COG subcomplexes with independent and functional lobes that influence the Golgi N-glycosylation independently. Lobe A is involved in maintaining the structural Golgi organization, whereas lobe B has a key role in B4GALT1 and ST6GAL1 stability.

Results

Steady-state level and intracellular distribution of B4GALT1 and ST6GAL1 in siCog3- and siCog7-transfected cells

To investigate the effects of either lobe A or lobe B of the COG complex on the Golgi localization and the steady-state level of both B4GALT1 and ST6GAL1, siRNA duplexes against Cog3p and Cog7p were designed to specifically mediate either lobe A or lobe B knockdowns of the COG complex. HeLa cells stably expressing either GalT1-GFP or SiaT1-GFP were shown to colocalize specifically with the cis-Golgi marker GM130 as indicated by the predominant yellow staining in the perinuclear region (Figure 1A and B, control). As shown in Figure 2, treatment of HeLa cells with siCog3 or Cog7 resulted in a substantial knockdown of their respective protein level by immunoblotting corresponding to a loss of 85–90% compared with untreated cells (Figure 2A). As published previously, we observed that Cog3p depletion was
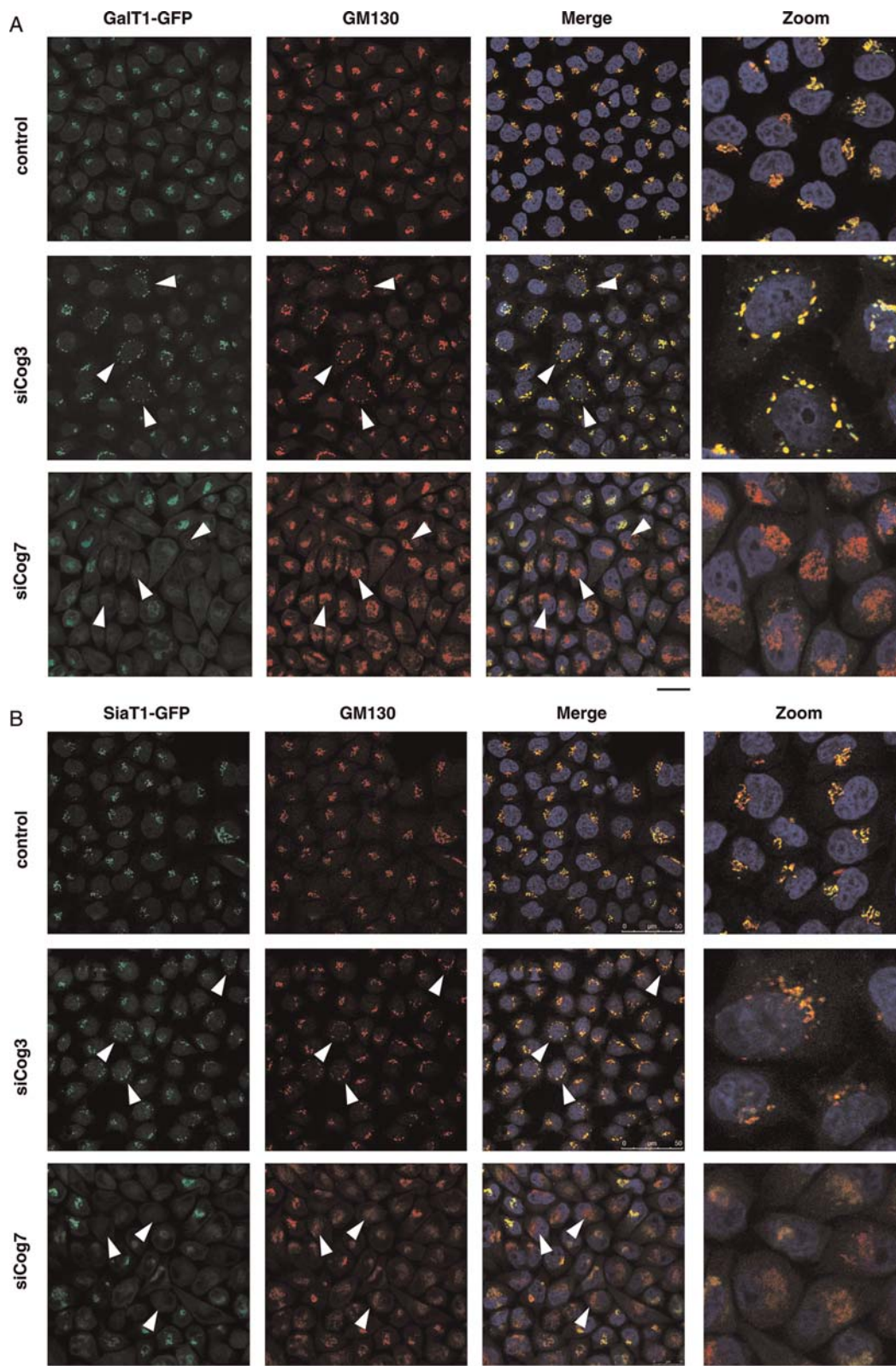
Fig. 1. Respective effects of siRNA induced COG3 KD (siCog3) and COG7 KD (siCog7) on Golgi morphology, steady-state levels and subcellular localization of B4GALT1 and ST6GAL1. HeLa cells stably expressing GalT1-GFP (**A**) and SiaT1-GFP (**B**) were transfected with either siCog3 or siCog7 at a concentration of 200 nM in the absence of fetal bovine serum. After 96 h, cells were fixed, stained with DAPI and analyzed by double immunofluorescence microscopy using the indicated primary antibody (GM130) and appropriate Alexa 568-conjugated secondary antibody. The images were collected with the same laser power and settings and processed with Adobe Photoshop 7.0. Scale bar represents 25 μm. Individual examples of transfected cells are indicated by arrowheads.
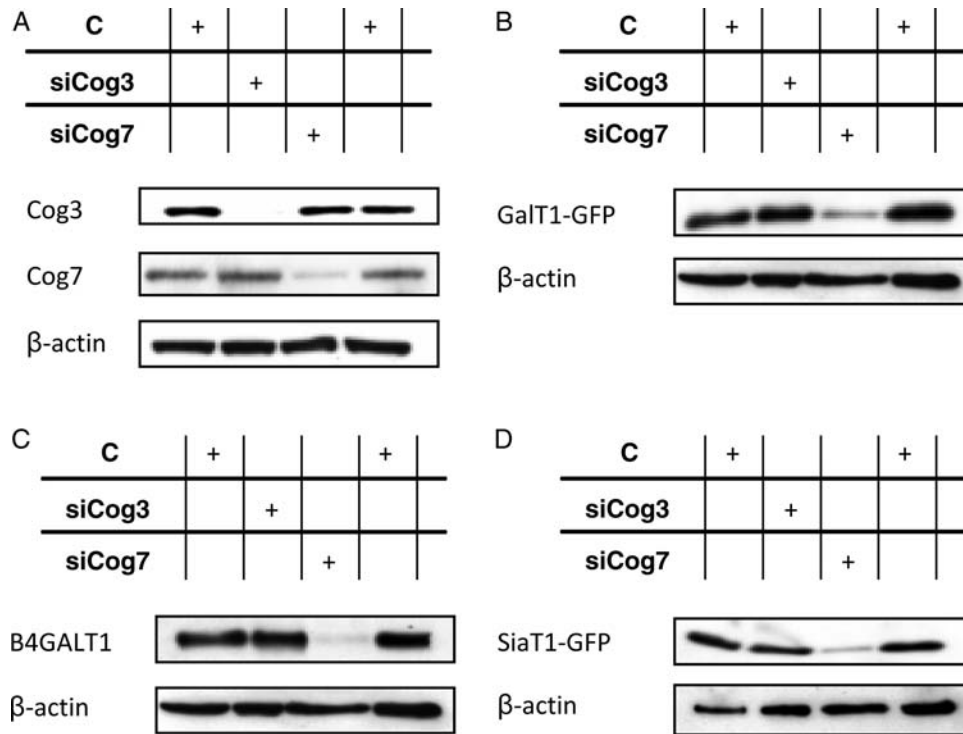
Fig. 2. COG7 KD affects the steady-state levels of B4GALT1 and ST6GAL1. (**A**) Control, siCog3 and siCog7 total cell extracts from HeLa WT cells were analyzed by immunoblotting using antibodies against the indicated COG subunits. (**B** and **C**) Control, siCog3 and siCog7 total cell extracts from HeLa cells stably expressing GalT1-GFP were immunoblotted with anti-GFP and anti-B4GALT1 as indicated. (**D**) Control, siCog3 and siCog7 total cell extracts from HeLa cells stably expressing SiaT1-GFP were analyzed by immunoblotting using anti-GFP antibody. Twenty micrograms of total cell extracts was loaded into each lane, and anti-β-actin antibody was used as a loading control.

accompanied by a clear reduction in the protein level of all lobe A subunits, whereas the protein level of lobe B subunits was unchanged (Zolov and Lupashin 2005; Sun et al. 2007). In contrast, Cog7p depletion was accompanied by reductions in the protein level of lobe B subunits whereas the protein level of lobe A subunits was unchanged (data not shown and Oka et al. 2005).

Compared with the normal Golgi ribbon observed in control cells (Figure 1A and B and Supplementary data, Figure S1B), Cog3p depletion resulted in a clear fragmentation of Golgi membranes with the appearance and accumulation of vesicles (Figure 1A and B and Supplementary data, Figure S1C). As shown by the colocalization study with two different Golgi markers (GM130 and GPP130), both GalT1-GFP and SiaT1-GFP were found distributed in these CCD Golgi structures named CCD vesicles by Lupashin and co-workers (Zolov and Lupashin 2005), demonstrating their ability to be relocated into CCD vesicles under Cog3p depletion (Supplementary data, Figure S1C).

Interestingly, a detailed analysis of siCog7-transfected cells did not reveal an accumulation of these two Golgi enzymes in CCD vesicles. Indeed, the steady-state level of both GalT1-GFP and SiaT1-GFP was dramatically reduced in Cog7p-depleted cells (Figure 1A and B), but without obvious alterations of the overall structure morphology of the Golgi, as indicated by the GM130 and the GPP130 stainings (Figure 1A and B, and Supplementary data, Figure S1D). In Cog7p-depleted cells, we noticed that the Golgi was less

fragmented, more compact and somewhat misshapen. Similarly and independently from the GFP tag, a severe alteration of its steady-state level was also observed for endogenous B4GALT1 (Supplementary data, Figure S1A). Thus, these results demonstrate that lobe B of the COG complex is crucial for the localization and the steady-state level of B4GALT1 and ST6GAL1. To further assess the stability of GalT1-GFP and SiaT1-GFP during Cog3p or Cog7p depletion, western blot assays using a mAb specific for GFP were performed (Figure 2B and D). No major decrease in both GalT1-GFP and SiaT1-GFP was observed in siCog3-treated cells. However, Cog7p depletion dramatically affected the steady-state level of both GalT1-GFP and SiaT1-GFP (Figure 2B and D). The same effect was observed on endogenous B4GALT1 (Figure 2C). To exclude any potential effects of siRNA-mediated Cog7p depletion on the mRNA level or stability of B4GALT1 and ST6GAL1, a QPCR-based approach was performed. Compared with control cells, the mRNA levels of B4GALT1 and ST6GAL1 were not significantly affected in Cog7p-depleted cells (Supplementary data, Figure S2A and B). Accordingly, these results allowed us to conclude that the observed alterations in the steady-state levels of B4GALT1 or ST6GAL1 in siCog7-transfected cells are not associated with any transcriptional regulation.

Altogether, our results strongly suggest that lobe B is crucial for the steady-state level of both B4GALT1 and ST6GAL1, whereas lobe A is necessary for maintaining the normal Golgi structure.
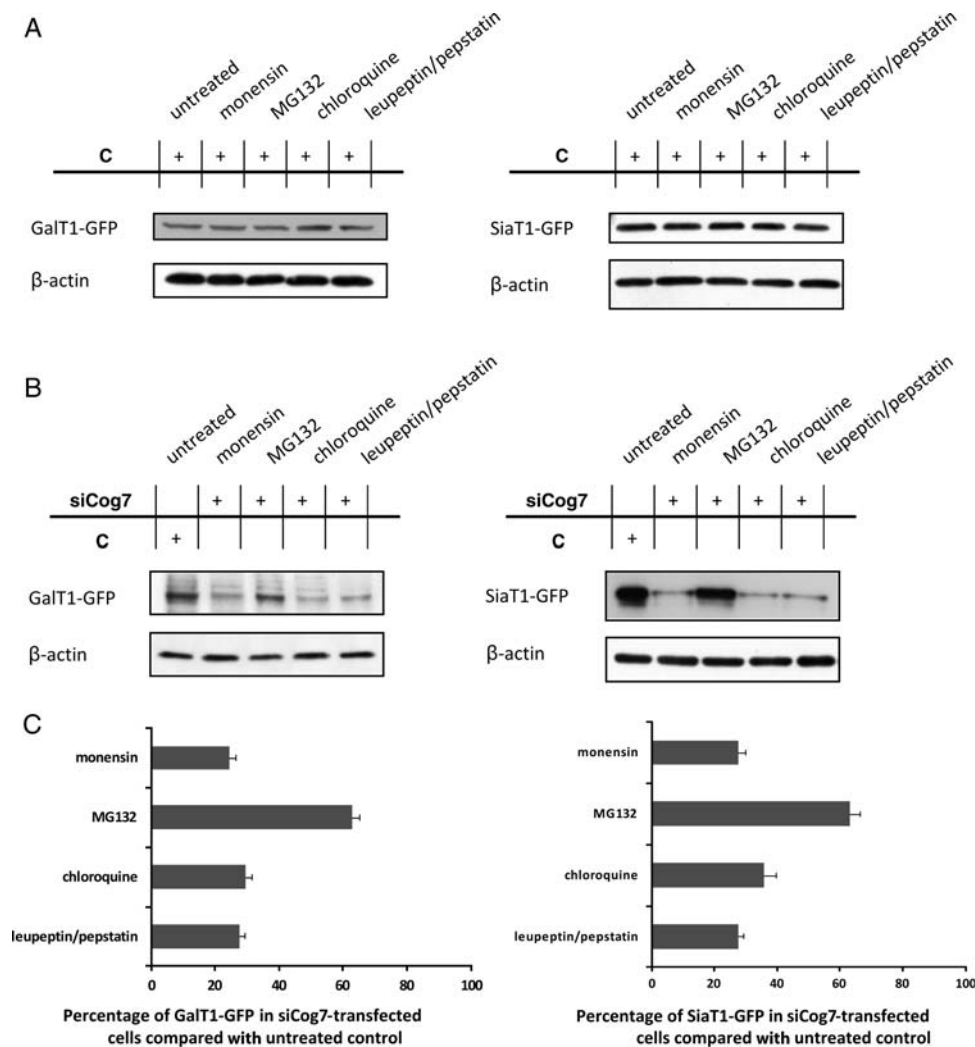
Fig. 3. Effects of proteasome and lysosome inhibitors on the steady-state levels of B4GALT1 and ST6GAL1 in control and siCog7-transfected cells. HeLa cells stably expressing GalT1-GFP (left) and SiaT1-GFP (right) were transfected with siCog7 at a concentration of 200 nM in the absence of fetal bovine serum. After 96 h, control (**A**) and siCog7-transfected (**B**) cells were treated with the indicated lysosomal and proteasomal inhibitors as described in the *Materials and Methods* section. Twenty micrograms of whole-cell lysates was analyzed by immunoblotting using anti-GFP antibody, and anti-β-actin antibody was used as a loading control. The abundance of the GalT1-GFP and the SiaT1-GFP in siCog7-transfected cells (lanes 2–5) treated with the indicated lysosomal and proteasomal inhibitors was compared with untreated control cells (lane 1) in (**C**). Quantifications represent the mean values of three independent loadings of three independent samples.

Effects of proteasome and lysosome inhibitors on B4GALT1 and ST6GAL1 stabilities

To assess the mechanism(s) by which GalT1-GFP and SiaT1-GFP could be degraded when cells were depleted for Cog7p, proteasomal and lysosomal inhibitors were used. To examine whether degradation of GalT1-GFP and SiaT1-GFP was mediated by the proteasomal pathway, cells were treated for 6 h with MG132, a specific proteasomal inhibitor. The GalT1-GFP and/or SiaT1-GFP were detected both by western blot assays and by immunofluorescence microscopy. Although Cog7p depletion was accompanied with a loss of GalT1-GFP and SiaT1-GFP in untreated cells (Figure 2B and D), treatment with MG132 significantly increased both GalT1-GFP and SiaT1-GFP protein levels by 62 ± 1.8 and $64 \pm 3.1\%$, respectively, compared with untreated control cells

(Figure 3B, lane 3, and C). Moreover, similar effects have been shown for the endogenous B4GALT1 (Supplementary data, Figure S2D), demonstrating that the effects of MG132 treatment on GalT1-GFP are not related to its overexpression. The steady-state rescue for these two Golgi glycosyltransferases was confirmed by immunofluorescence microscopy, as indicated by the predominant green staining in the perinuclear region observed after MG132 treatment (Figure 4A and B). Therefore, both GalT1-GFP and SiaT1-GFP were shown to colocalize specifically with the Golgi marker giantin (Figure 5A and B). Hence, this demonstrated that the MG132 treatment was not only able to rescue the steady-state levels of GalT1-GFP and SiaT1-GFP but also their Golgi localization. In contrast, by using the lysosomal inhibitors pepstatin A and leupeptin in siCog7-treated cells, no effects either on the
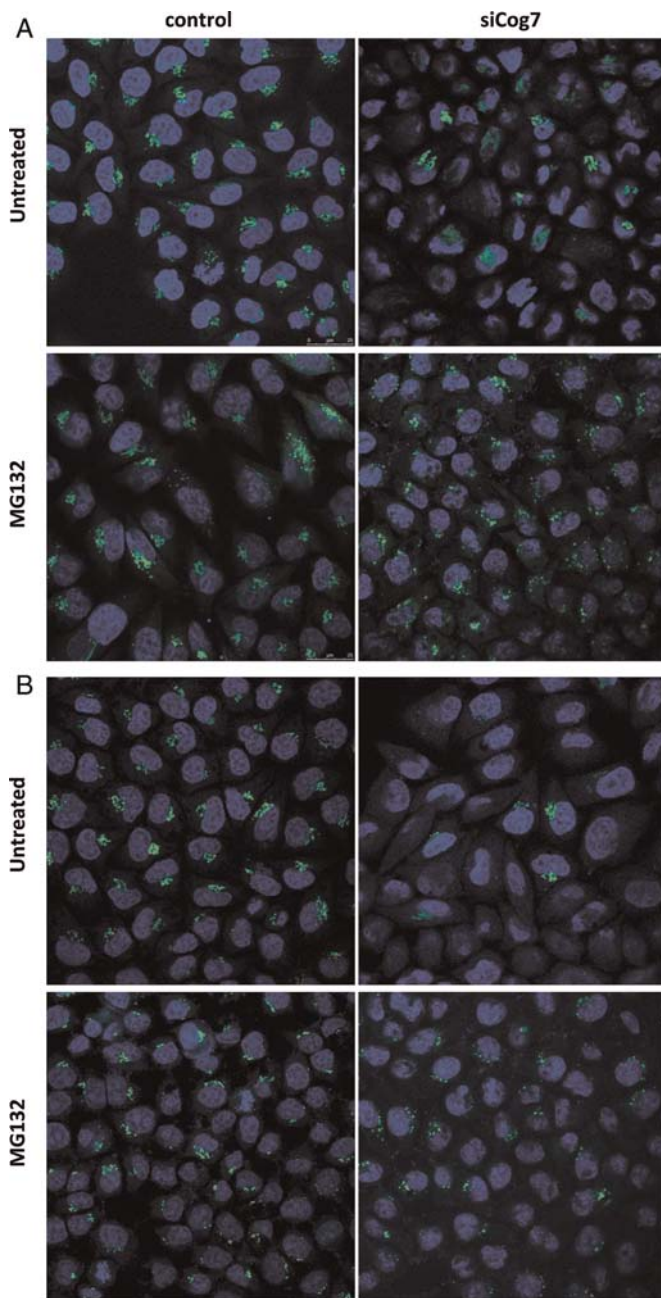
Fig. 4. Effects of the proteasome inhibitor MG132 on the subcellular localization rescue of B4GALT1 and ST6GAL1 in control and siCog7-transfected cells. HeLa cells stably expressing GalT1-GFP (**A**) and SiaT1-GFP (**B**) were transfected with siCog7 at a concentration of 200 nM in the absence of fetal bovine serum. After 96 h, cells were treated with MG132 as described in the *Materials and Methods* section, then fixed and stained with DAPI for analysis by immunofluorescence microscopy. The images were collected with the same laser power and settings and processed with Adobe Photoshop 7.0. Scale bar represents 25 μm.

GalT1-GFP and SiaT1-GFP levels (Figure 3B, lane 5) or on their Golgi localization (Supplementary data, Figure S3A and B) were observed. To exclude that the stabilization of GalT1-GFP and SiaT1-GFP by the MG132 treatment was not

mediated by the Cog7p rescue, western blot assays with pAb against Cog7p were performed in control and siCog7-transfected cells treated with or without MG132. As shown in supplemental data (Figure S2C), treatment with MG132 had no effects on the protein level of Cog7p in siCog7-transfected HeLa cells.

We then examined whether an alternative method to inhibit lysosomal protease activity, by preventing the acidification of the endosomal/lysosomal system, could rescue the steady-state levels of GalT1-GFP and SiaT1-GFP in siCog7-treated cells. The acidification was inhibited using the lysosomotropic weak base chloroquine diphosphate and the carboxylic ionophore monensin (see de Duve et al. 1974 for review). SiCog7-transfected cells were treated with either chloroquine or monensin, and the steady-state levels were analyzed by western blot assays and by immunofluorescence microscopy. As observed in Figure 3B (lanes 2 and 4) and Supplementary data, Figure S3, lysosomal inhibition by either chloroquine or monensin had no effects on the rescue steady-state levels and subcellular localization of GalT1-GFP and SiaT1-GFP.

Furthermore, the stability and/or localization of GalT1-GFP and SiaT1-GFP in control cells after treatment with lysosome inhibitors were checked, and as revealed by immunofluorescence analysis, no major differences were observed compared with untreated cells (Supplementary data, Figure S3A and B). Taken together, these results allowed us to conclude that the observed degradation of GalT1-GFP and SiaT1-GFP in Cog7p-depleted cells was mediated by the proteasome pathway.

Analysis of glycosylation defects in lobe A- and lobe B-depleted cells

To highlight the Golgi *N*-glycosylation defects in lobe A and lobe B depleted cells, various FITC-conjugated lectins were used for flow cytometry analysis. For this study, the high-mannose structures specific lectin concanavalin A (ConA), the *Sambucus nigra* agglutinin (SNA) that binds to sialic acid terminally linked α(2–6) to galactose or *N*-acetylgalactosamine residues, and the wheat germ agglutinin (WGA) that binds terminal GlcNAc residues were used. In order to validate lectin-binding specificity, complementary competitive sugars that are known to block lectin binding were used (Supplementary data, Figure S4). Figure 6 shows histogram plots of control (Figure 6A), siCog3-transfected (Figure 6B) and siCog7-transfected (Figure 6C) HeLa cells incubated with FITC-labeled SNA and analyzed for SNA binding. For each histogram, the fluorescence peak corresponding to SNA binding in the presence of 200 mM lactose (nonspecific binding) is represented. Specific binding was calculated as the difference between the mean fluorescence intensities of total and nonspecific peaks. Weak fluorescence intensity shifts for nonspecific SNA binding were observed for siCog3- and siCog7-transfected cells in comparison to control HeLa cells. These shifts were attributed to slight morphological changes in cells, consecutive to the siRNA transfection, as assessed by the FSC/SSC dot plot (data not shown). As presented in Figure 6A, two distinct populations of cells were observed in control HeLa cells. A very minor population (left peak) was shown to overlay with
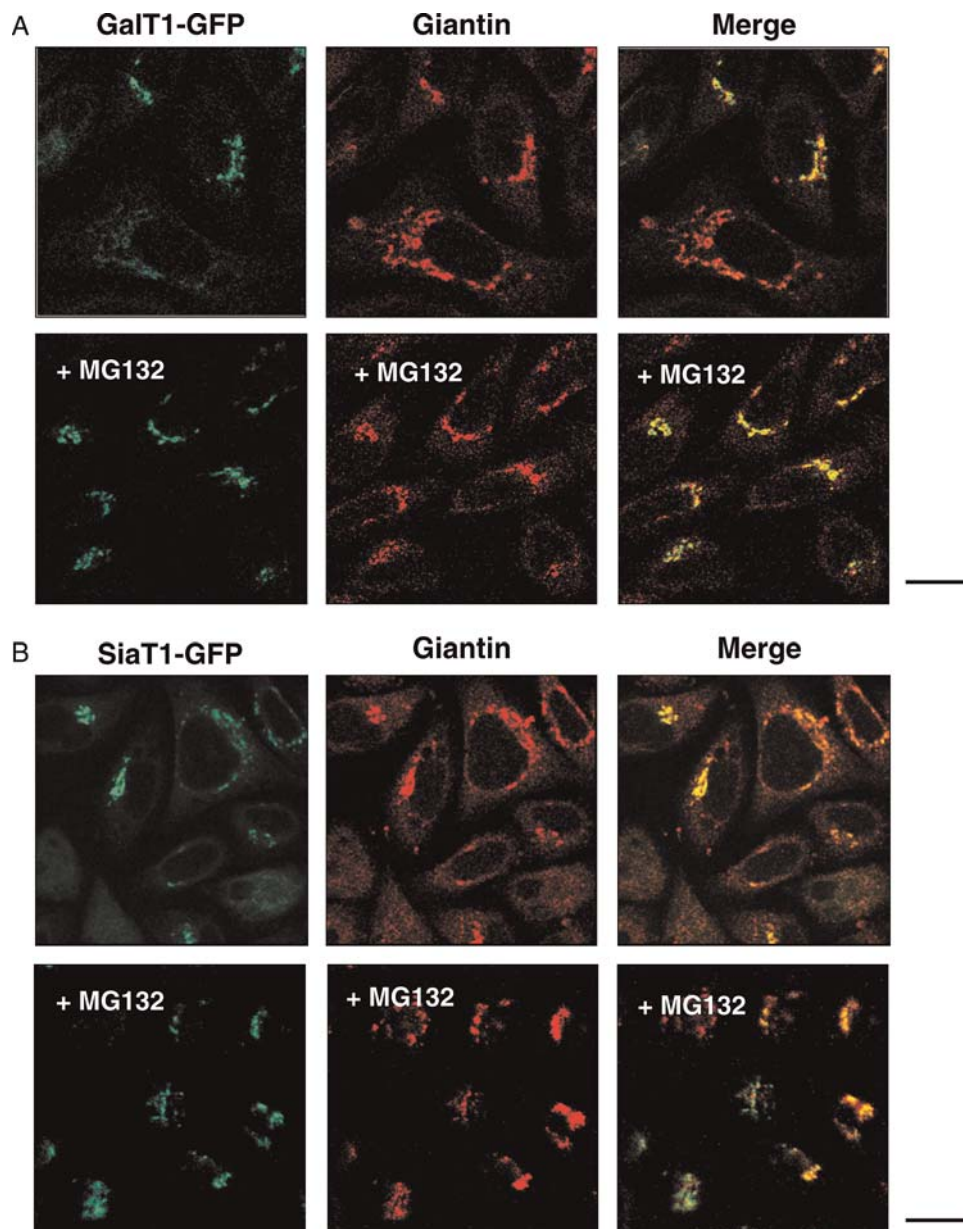
Fig. 5. MG132 induced rescue on Golgi subcellular localization of GalT1-GFP and SiaT1-GFP. HeLa cells stably expressing GalT1-GFP (**A**) and SiaT1-GFP (**B**) were transfected with siCog7 at a concentration of 200 nM in the absence of fetal bovine serum. After 96 h, cells were treated or not treated with MG132, then fixed and analyzed by double immunofluorescence microscopy with the Golgi marker giantin. The images were collected with the same laser power and settings and are processed with Adobe Photoshop Elements 7.0. Scale bar represents 25 μm.

neuraminidase-treated HeLa cells, which most likely corresponds to cells presenting desialylated glycan structures. In siCog7-transfected cells (Figure 6C), this population represented more than 42% of total cells and is characterized by a loss of more than 97% of specific SNA binding. siCog3-transfected cells (Figure 6B) showed an intermediate fluorescence pattern between control (Figure 6A) and Cog7p-depleted cells (Figure 6C). Binding of ConA and WGA lectins was also analyzed for control, siCog3-transfected and siCog7-transfected cells (Figure 6D). Owing to the weak fluorescence intensity differences between

the total and the nonspecific peaks, which do not allow to discriminate within the two populations (data not shown), the results were expressed as percentages of specific lectin binding to cells. In the calculation, specific lectin binding to control cells, which corresponds to the difference between the total and the nonspecific peaks, was considered as 100%. As shown in Figure 6D, ConA binding did not evidence obvious differences between control and siRNA-transfected cells. This demonstrates that neither Cog3p nor Cog7p depletion affects the early *N*-glycosylation steps. In contrast, a strong enhancement for WGA-specific binding was observed in siCog3- and
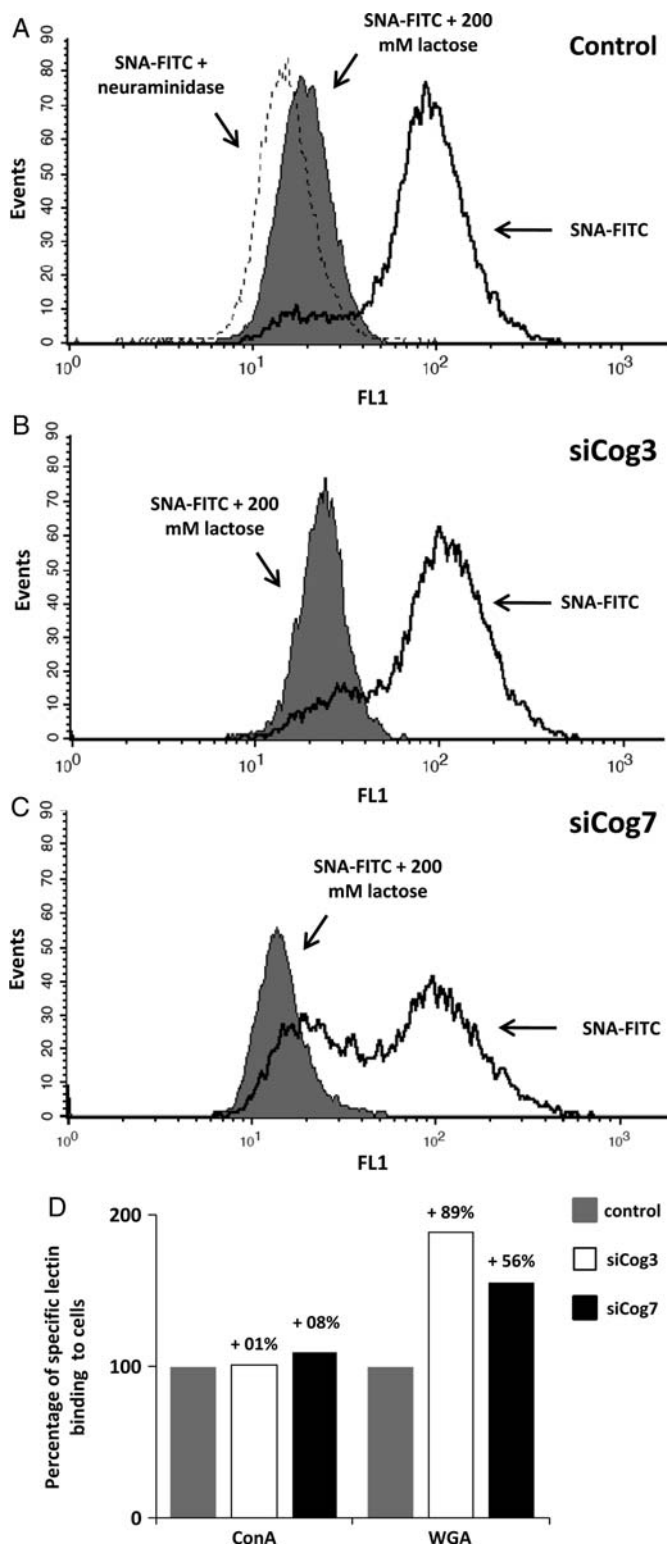
Fig. 6. Analysis of glycosylation defects in control, siCog3-transfected and siCog7-transfected cells by lectin staining and fluorescence flow cytometry. HeLa WT cells were transfected with either siCog3 or siCog7 at a concentration of 200 nM in the absence of fetal bovine serum. After 96 h, cells were harvested, fixed, permeabilized and incubated with FITC-conjugated lectins for flow cytometry analysis, as described in the *Materials and Methods* section. Histogram plots of control (**A**),

siCog7-transfected cells (+89 and +56%, respectively). These observations clearly indicate moderate and severe abnormalities in the terminal Golgi glycosylation for Cog3p- and Cog7p-depleted cells, respectively.

COG sensitivity of a set of Golgi proteins

In order to determine whether the differential effects of lobe A and lobe B of the COG complex on protein stability was only observed for B4GALT1 and ST6GAL1, we analyzed the effects of the depletion of the Cog3 or the Cog7 subunit, on a subset of Golgi-associated proteins by western blot (Figure 7). Proteins tested for a potential reduction or increase in their steady-state levels in the Cog3- and/or Cog7-depleted cells were αβSNAP, CASP, Exo70, GPP130, GS15, GS28 and ZW10. Some are resident Golgi transmembrane proteins previously referred to GEARs: the golgin CASP, the Golgi phosphoprotein GPP130 and the SNARE protein GS15 (Oka et al. 2004). GPP130 is a glycoprotein of unknown function, whose location in the Golgi is sensitive to changes in intraluminal pH (Linstedt et al. 1997; Puri et al. 2002). The steady-state level of both GPP130 and the exocytic intermediate protein Exo70 was noticeably altered consecutively to the loss of both lobe A and lobe B function. These proteins exhibited an alteration of −20 and −11%, respectively, in their steady-state level due to the loss of lobe A of the COG complex and of −17 and −39%, respectively, after the disruption of lobe B. Similarly, the protein GS15 was the only SNARE protein to present a significantly decreased expression (−31%) due to the loss of the lobe B function and a slight alteration (−7%) in its steady-state level after the disruption of the lobe A of the COG complex. Inversely, some proteins appeared overexpressed in response to siCog3 or siCog7. The expression of GS28 was indeed enhanced by 8 and 24% following the loss of lobe A and lobe B function, respectively. Loss of the lobe B of the COG complex was accompanied with a 15% increase in the expression of αβSNAP, whereas CASP and ZW10 proteins presented slight increases in their steady-state level following the loss of lobe A of the COG complex.

Discussion

Many studies have highlighted the crucial role of the hetero octameric COG complex in establishing or maintaining the

siCog3-transfected (**B**) and siCog7-transfected (**C**) HeLa cells analyzed for SNA binding and incubated with FITC-labeled SNA (total binding, black tracing) are shown. For each histogram, the fluorescence peak corresponding to SNA binding in the presence of 200 mM lactose is represented (nonspecific binding, grey fill). Specific binding was calculated as the difference between the mean fluorescence intensities of total and nonspecific-binding peaks. Desialylation was performed before the incubation with lectins, using type V neuraminidase from *Clostridium perfringen*s. One representative experiment from a set of three independent experiments is shown. In A, the SNA binding of neuraminidase-treated cells is also depicted (dotted line). Binding of ConA and WGA lectins was also analyzed for control (grey), siCog3-transfected (white) and siCog7-transfected (black) cells in **D**. The results were expressed as the percentages of specific lectin binding to cells. In the calculation, specific lectin binding to control cells, which corresponds to the difference between the total and the nonspecific-binding peaks, was considered as 100%. One representative experiment from a set of three independent experiments is illustrated.

normal structure and functions of the Golgi apparatus (Oka et al. 2004; Zolov and Lupashin 2005; Shestakova et al. 2006). Over the past 5 years, mutations in COG complex subunits have been identified in CDG-II patients and all are associated with defects in glycoconjugate synthesis, in the stability and localization of resident Golgi proteins, in the ultrastructure of the Golgi apparatus and in retrograde intra-Golgi trafficking (Wu et al. 2004; Spaapen et al. 2005; Foulquier et al. 2006; Steet and Kornfeld 2006; Foulquier et al. 2007; Kranz et al. 2007; Ng et al. 2007; Paesold-Burda et al. 2009; Reynders et al. 2009). Strikingly, differential effects in late Golgi glycosylation (sialylation and galactosylation) on total serum N-glycoproteins were observed depending on the affected subunits (Foulquier et al. 2007; Kranz et al. 2007; Reynders et al. 2009). This led us to hypothesize that individual COG subunits or subcomplexes may play distinct roles in controlling stability and/or Golgi localization of late Golgi glycosyltransferases. To address this point, a siRNA strategy on Cog3 and Cog7 subunits, for a respective knockdown of the lobe A and the lobe B of the COG complex in HeLa cells stably expressing GFP-tagged B4GALT1 and ST6GAL1, was used.

In the current study, we have characterized the consequences of the loss of either lobe A or lobe B on the steady-state levels and localization of the two major Golgi glycosyltransferases involved in terminal N-linked glycosylation. We could establish that the acute depletion of the Cog3 subunit of the COG complex resulted in dramatic changes in the Golgi structure, but did not have an effect on the steady-state levels of GalT1-GFP and SiaT1-GFP. In contrast, we demonstrated that the depletion of Cog7p severely altered the stability of these two late Golgi glycosylation enzymes.

As already observed by Zolov and Lupashin (2005), Cog3p depletion was associated with a clear fragmentation of Golgi membranes leading to the appearance of CCD vesicles where both GalT1-GFP and SiaT1-GFP were found to accumulate in these structures. In contrast, immunofluorescence analysis of siCog7-transfected cells did not show an accumulation of these two Golgi enzymes in CCD vesicles, but rather resulted in a dramatic alteration of their steady-state levels. Similarly and independently from the GFP tag, a complete instability was also observed for the endogenous B4GALT1 under these conditions. The steady-state levels of GalT1-GFP and SiaT1-GFP under COG3 and COG7 KD were further assessed by western blot analysis. As expected and in agreement with the obtained immunofluorescence data, no major decrease in both enzymes was observed in Cog3p-depleted cells. However, in siCog7-transfected cells, an 85% decrease in the protein level was observed for both GalT1-GFP and SiaT1-GFP. Given that Cog7p depletion affects the entire stability of the lobe B of the COG complex, our results clearly point out that lobe B is crucial for the steady-state levels of B4GALT1 and ST6GAL1. We then focused our study on the mechanism of GalT1-GFP and SiaT1-GFP degradation under Cog7p depletion. We demonstrated that lysosomal inhibition by either pepstatin A/leupeptin, chloroquine or monensin had no effects on the rescue levels of GalT1-GFP and SiaT1-GFP. However, treatment with the proteasome inhibitor MG132 significantly restored both GalT1-GFP and SiaT1-GFP

steady-state levels but also their Golgi localization. These results therefore suggest that the degradation of GalT1-GFP and SiaT1-GFP under siCog7 is likely the consequence of a fast redistribution of these proteins into the ER, immediately followed by a retrotranslocation into the cytosol and the proteasomal degradation. Similar results have been observed in ldlB and ldlC CHO cells by Oka et al. (2004) for a set of integral membrane Golgi proteins called GEARs. In mutant cells, GEARs proteins were found abnormally localized in the ER and degraded by proteasomes. However, in contrast to the work of Oka et al., we did not observe an increased amount of the MG132-induced accumulation of GalT1-GFP and SiaT1-GFP in the ER. Indeed, the observed Golgi rescue in the GalT1-GFP and the SiaT1-GFP localization following MG132 treatment suggests that lobe B KO most likely does not affect efficient ER exit and anterograde vesicular Golgi trafficking.

The molecular mechanisms by which the lobe B affects the distribution of these two Golgi glycosyltransferases are unknown but our results suggest that the lobe B would be crucial in preventing these Golgi glycosyltransferases from inappropriate retrograde trafficking to the ER. Finally, the analysis of glycosylation defects in both lobe A- and lobe B-depleted cells was achieved by flow cytometry analysis by using FITC-conjugated lectins. We clearly demonstrated that alterations in the late steps of N-linked oligosaccharide processing are independent of the affected lobes. However, deeper abnormalities were associated with lobe B depletion.

To go further and discriminate with the functions of lobe A and lobe B of the COG complex, we examined the effects of efficient knockdown of the Cog3 and Cog7 subunits, respectively, on a subset of Golgi-associated proteins. Interestingly, the subsequent loss of lobe A or lobe B function had different effects on the steady-state level of some of the tested secretory-pathway-related proteins suggesting that the observed effect was not limited to B4GALT1 and ST6GAL1. The Golgi phosphoprotein GPP130, the exocytic intermediate protein Exo70 and the SNARE protein GS15 were the only proteins we found whose steady-state levels were noticeably altered due to the loss of either lobe of the COG complex. On the contrary, the expression of the other COG sensitive proteins was either enhanced or reduced following acute knockdown of either lobe A or lobe B of the COG complex. Concerning proteins of the intracellular trafficking machinery, inactivation of the function of the lobe B of the COG complex was mainly associated with variations in the steady-state levels of the SNARE proteins GS15 and GS28. Both GS15 and GS28 were shown to form a SNARE complex with Syntaxin 5 with implications for intra-Golgi transport (Xu et al. 2002) and in early/recycling endosome to the TGN retrograde trafficking steps (Tai et al. 2004). Genetic and physic interactions of the COG complex with Golgi SNARE molecules and the vesicle coat complex COPI in the retrograde intra-Golgi trafficking were additionally described in yeast (Ram et al. 2002; Suvorova et al. 2002). The described interaction of several COG subunits with the yeast SM (Sec1/Munc18) protein Sly1 further supported the hypothesis that this complex might be involved not only in SNARE stability, but also in promoting vesicular fusion by stabilizing the final SNARE complex (Shestakova et al. 2007).
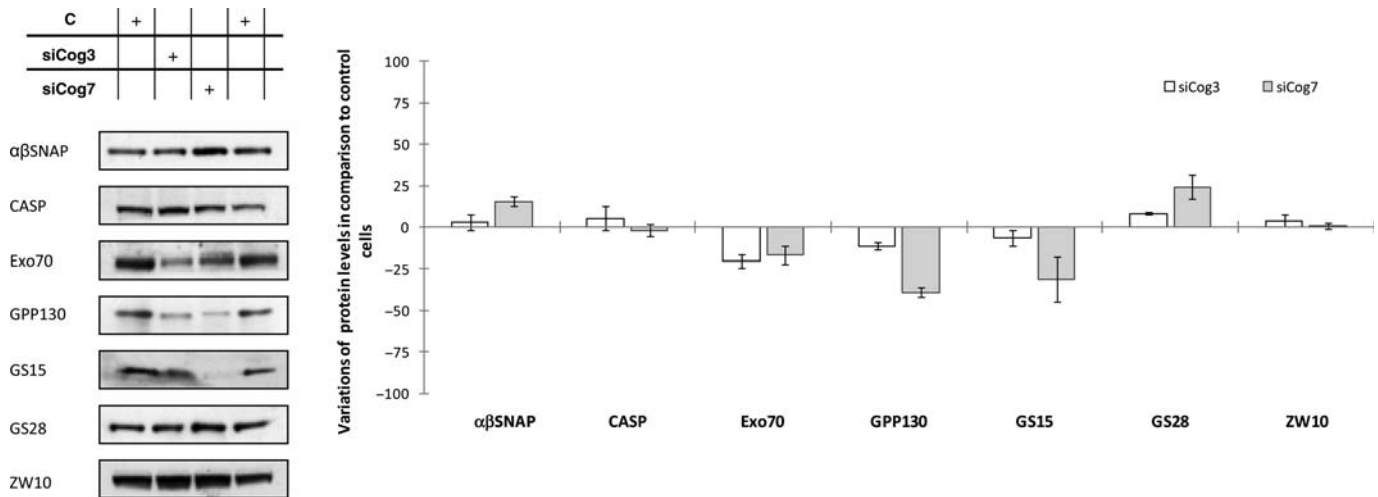
Fig. 7. Analysis of the COG sensitivity of a set of Golgi proteins in siCog3- and siCog7-transfected cells. Total cell extracts from control, siCog3-transfected and siCog7-transfected HeLa cells were analyzed by immunoblotting using antibodies to the indicated Golgi-related proteins. Twenty micrograms of total cell extracts was each time loaded, and anti-β-actin antibody was used as a loading control. Quantifications represent the mean values of three independent loadings of three independent samples for both COG3 and COG7 KD.

In conclusion, our results emphasize for the first time an independent and differential role of lobe A and lobe B COG subcomplexes for the stability and localization of trans-Golgi enzymes. Both lobes are clearly required for efficient terminal Golgi glycosylation, and the depletion of either lobe A or B leads to moderate to severe Golgi glycosylation defects. In addition, lobe A and lobe B differently affect the localization and stability of two late Golgi glycosyltransferases B4GALT1 and ST6GAL1. Our results then suggest that lobe A KD likely affects the Golgi glycosylation by leading to a mislocalization of trans-Golgi glycosyltransferases in CCD vesicles then preventing the Golgi glycosyltransferases to be in contact with the cargo molecules that need to be glycosylated. At the opposite, the dramatic effects of lobe B KD on terminal Golgi glycosylation result from the complete loss of B4GALT1 and ST6GAL1. These results are in good agreement with the different glycosylation abnormalities observed in the sera of COG-deficient CDG-II patients.

Materials and methods
Cell culture and other reagents
Cell culture reagents were purchased from Lonza (Levallois-Perret, France). HeLa cells stably expressing GalT1-GFP and SiaT1-GFP enzymes were grown in DMEM supplemented with 10% fetal calf serum and 2.5 mM L-glutamine (DMEM/FCS) at 37°C and 5% CO_2 in a humidified chamber. The proteasome and lysosome inhibitors monensin (2 μM, 2 h), MG132 (8 μM, 6 h), chloroquine (10 μM, 24 h), leupeptin (50 μM, 24 h) and pepstatin (1 μM, 24 h) were from Sigma-Aldrich (St Louis, MO) and were investigated at the respective concentrations and incubation times given in brackets. Subconfluent monolayers were incubated in the DMEM/FCS medium to which the agents were added immediately before the experiment to the suitable final concentrations, whereas controls were incubated with the same volumes of fresh medium and solvent.

Antibodies
Affinity-purified or crude serum rabbit polyclonal antibodies (pab) were used against the Cog3 and Cog7 subunits in dilutions 1:1000 for western blotting. Pab against Cog3 and B4GALT1 (1:250 for indirect immunofluorescence and 1:750 for western blotting) were gifts from V. Lupashin (University of Arkansas for Medical Sciences, Little Rock) and E. G. Berger (University of Zürich, Zürich, Switzerland), respectively. Mab anti-GM130 (1:100 for indirect immunofluorescence) and anti-GS15 (1:500 for western blotting) were from BD Biosciences (Franklin Lanes, NJ). Mab anti-GFP (1:1000 for western blotting) was from Sigma-Aldrich. Both anti-giantin (1:1000 for indirect immunofluorescence) and anti-GPP130 (1:500 for western blotting) pab were from Covance (Richmond, CA). Various antibodies used in Figure 7 were gifts from different laboratories.

Immunoblotting
Twenty micrograms of proteins was analyzed by SDS–PAGE and immunoblotted with the indicated antibodies at the concentrations described previously. Cells were rinsed twice with ice-cold phosphate-buffered saline (PBS) and then lysed for 5 min on ice in cell lysis buffer (25 mM Tris–HCl, 150 mM NaCl, pH 7.6, supplemented with 1% Triton X-100, 1% sodium deoxycholate and 0.1% SDS). Proteins were quantified by using the Micro BCA Protein Assay Kit (Thermo Fisher Scientific, Brebieres, France). Signals were detected using the ECL Plus Detection Kit (Amersham Biosciences, UK) according to the manufacturer's instructions. Signal detection was performed by autoradiography and quantified with the GS800 Calibrated Imaging Densitometer (Bio-Rad Laboratories, UK), using the Quantity One software for image acquisition and analysis.

Immunofluorescence staining
Cells were grown on glass coverslips, washed once with PBS and fixed by incubation for 30 min with 4%

873

paraformaldehyde in 0.1 M sodium phosphate buffer (pH 7.2) at room temperature. The coverslips were rinsed three times with PBS for 5 min. The fixed cells were permeabilized with PBS containing 0.5% Triton X-100 for 5 min and washed three times with PBS. The fixed cells were then incubated for at least 60 min with a blocking solution containing 0.1% Triton X-100 (Sigma-Aldrich), 1% BSA (Roche Applied Science) and 5% normal goat serum (Invitrogen) in PBS. After blocking, the cells were incubated overnight at 4°C with primary antibodies diluted in the blocking solution as described previously. The cells were then washed again three times in PBS, followed by incubation with the Alexa 488- or Alexa 568-conjugated secondary antibodies (1:500, Invitrogen) for 1 h at room temperature in dark. Cells were then post-stained with 500 ng mL^{-1} DAPI (Sigma-Aldrich) for 5 min to detect cell nuclei, and washed three times with PBS. Immunostaining was detected through an inverted Leica SP5 spectral microscope (IRI CNRS USR 3078, Villeneuve d'Ascq, France) with a 63× oil immersion lens at room temperature. Data were therefore collected using the LAS 6000 AF software and finally processed in Adobe Photoshop 7.0 (Adobe Systems, San Jose).

Lectin binding and flow cytometry assay

Control, siCog3-transfected and siCog7-transfected cells were harvested in 2 mM EDTA for 15 min at room temperature, fixed with 4% PFA in PBS on ice for 30 min, and then incubated in 50 mM NH$_4$Cl on ice for 15 min. After two washes with PBS, cells were permeabilized with 0.3% saponin and 0.1% BSA for 15 min at 4°C. Cells were then washed once in PBS and resuspended to final concentration of 1×10^6 cells mL^{-1} in PBS containing 0.1% BSA. All washing and incubation steps were carried out in the BSA solution. Desialylation was performed before the incubation with lectins, using 50 mU of type V neuraminidase from Clostridium perfringens (Sigma-Aldrich) in 50 mM sodium acetate buffer, 0.9% NaCl, 0.1% CaCl$_2$, 1% BSA, pH 5.0, for 3 h at 37°C. Twenty micrograms of FITC-labeled lectins from stocks solutions of lectins of concentration 2 and 5 mg mL^{-1} was added to 50 µL cell suspension aliquots of 5×10^4 cells. All lectins were purchased from Vector Laboratories (Burlingame, CA). Final volumes were made up to 150 µL. Incubations were carried out in the dark for 30 min with occasional agitation. In addition, the degree of specificity of lectin binding was determined by incubation with appropriate monosaccharide inhibitors. These adequate competitive sugars were preincubated with lectins for 1 h prior to addition of cells. The FITC-labeled lectins and corresponding sugar inhibitors were: the ConA which specifically binds to α-linked Man residues or terminal Glc and is inhibited with 200 mM α-methylmannoside; the SNA which binds to α2,6-linked NeuAc residues and is inhibited with 200 mM Lac; and finally, the WGA which binds to β1,4-linked GlcNAc residues and is inhibited with 100 mM GlcNAc.

Flow cytometry analysis was performed on a Becton-Dickinson FACSCalibur flow cytometer (Le-Pont-De-Claix, France). Immediately after incubation with lectins, cells were resuspended in 500 µL of Isoton solution (Becton-Dickinson, Le-Pont-De-Claix) and submitted to cytometry analysis. Each analysis was performed on at least 10,000–20,000 cells gated on the region of the HeLa cells population, based on light scatter properties (forward versus side: FSC/SSC). Fluorescence intensity data from the FL1 (green fluorescence) channel were collected and analyzed using the Cell Quest Pro software.

RNA interference experiment

Microsynth Laboratory (Balgach, Switzerland) manufactured all siRNAs. Both siCog3 and the two Stealth siCog7 duplex sequences have been published previously by the Lupashin laboratory (Zolov and Lupashin 2005; Shestakova et al. 2006). Duplexes were transfected at a final concentration of 200 nM by using Lipofectamine 2000 (Invitrogen) according to the manufacturer's instructions with slight modifications. Cells were tranfected in OptiMEM medium, in the absence of fetal bovine serum. Two cycles of siRNA were done to achieve maximal knockdown, every 48 h. Cells were transfected with corresponding siRNAs and collected for analysis 96 h later.

Real-time reverse transcriptase–PCR

Total RNA was isolated using the Nucleospin RNA II Kit (Macherey Nagel, Hoerdt, France). The amount of extracted RNA was quantified using a NanoDrop spectrophotometer (Thermo Scientifics, Wilgminton, DE) and the purity of RNA was checked by the ratio of the absorbance at 260 and 280 nm. Two micrograms of purified total RNA was then subjected to reverse transcription with the First-Strand cDNA Synthesis Kit (GE Healthcare), following the manufacturer's instructions. For PCRs, cDNAs obtained after reverse transcription were diluted 1:5. PCRs were performed for the B4GALT1 (GenBank NM_001497) and ST6GAL1 (GenBank NM_003032) genes and for the house-keeping gene HPRT (Hypoxanthine PhosphoRibosylTransferase, GenBank NM_000194), which was used as an endogenous control for normalization. PCR primers were designed using Primer 3 software (http://frodo.wi.mit.edu). All the primers were synthesized by Eurogentec (Seraing, Belgium). PCR primers used are the following: B4GALT1 (5′-GCAAAGCAGAACC CAAATGT-3′ and 5′-GCAAAGCAGAACCCAAATGT-3′), ST6GAL1 (5′-GGCATCAAGTTCAGTGCAGA-3′ and 5′-TG CGTCATGATCATCGATTT-3′) and HPRT (5′-GCCAGACTT TGTTGGATTTG-3′ and 5′-CTCTCATCTTAGGCTTTGTAT TTTG-3′). PCRs (25 µL) were performed using 2X SYBR® Green Universal QPCR Master Mix (Stratagene, Amsterdam, The Netherlands) with 2 µL of a 1:5 cDNA dilution and 300 nM final concentration of each primer. Data were analyzed using the MX4000 PCR system software (Stratagene). To quantify the results, we used the comparative threshold cycle method described by Livak and Schmittgen (2001). Serial dilutions were used to create standard curves for relative quantification, and glycosyltransferases transcripts were normalized to HPRT expression.

Supplementary data

Supplementary data for this article are available online at http://glycob.oxfordjournals.org/.

Funding

Conflict of interest

None declared.

Acknowledgements

Abbreviations

B4GALT1, β1,4-galactosyltransferase 1; CCD, COG complex-dependent; CDG, congenital disorders of glycosylation; CHO, Chinese hamster ovary; COG, conserved oligomeric Golgi; ConA, concanavalin A; ER, endoplasmic reticulum; GFP, green fluorescent protein; MAB, monoclonal antibody; PAB, polyclonal antibody; PBS, phosphate-buffered saline; QPCR, quantitative polymerase chain reaction; SNA, *Sambucus nigra* agglutinin; siRNA, small-interfering RNA; ST6GAL1, α2,6-sialyltransferase 1; WGA, wheat germ agglutinin.

References

de Duve C, de Barsy T, Poole B, Trouet A, Tulkens P, Van Hoof F. 1974. Commentary. Lysosomotropic agents. *Biochem Pharmacol.* 23:2495–2531.

Elsner M, Hashimoto H, Nilsson T. 2003. Cisternal maturation and vesicle transport: Join the band wagon! *Mol Membr Biol.* 20:221–229.

Ferrari MC, Parini R, Di Rocco MD, Radetti G, Beck-Peccoz P, Persani L. 2001. Lectin analyses of glycoprotein hormones in patients with congenital disorders of glycosylation. *Eur J Endocrinol.* 144:409–416.

Fotso P, Koryakina Y, Pavliv O, Tsiomenko AB, Lupashin VV. 2005. Cog1p plays a central role in the organization of the yeast conserved oligomeric Golgi complex. *J Biol Chem.* 280:27613–27623.

Foulquier F. 2009. COG defects, birth and rise! *Biochim Biophys Acta.* 1792:896–902.

Foulquier F, Ungar D, Reynders E, Zeevaert R, Mills P, García-Silva MT, Briones P, Winchester B, Morelle W, Krieger M, et al. 2007. A new inborn error of glycosylation due to a Cog8 deficiency reveals a critical role for the Cog1-Cog8 interaction in COG complex formation. *Hum Mol Genet.* 16:717–730.

Foulquier F, Vasile E, Schollen E, Callewaert N, Raemaekers T, Quelhas D, Jaeken J, Mills P, Winchester B, Krieger M, et al. 2006. Conserved oligomeric Golgi complex subunit 1 deficiency reveals a previously uncharacterized congenital disorder of glycosylation type II. *Proc Natl Acad Sci USA.* 103:3764–3769.

Helenius A, Aebi M. 2004. Roles of N-linked glycans in the endoplasmic reticulum. *Annu Rev Biochem.* 73:1019–1049.

Jaeken J, Vanderschueren-Lodeweyckx M, Casaer P, Snoeck L, Corbeel L, Eggermont E, Eeckels R. 1980. Familial psychomotor retardation with markedly fluctuating serum prolactin, FSH, and GH levels, partial TBG deficiency, increased arylsulfatase A and increase CSF protein: A new syndrome? *Pediatr Res.* 14:179.

Kornfeld R, Kornfeld S. 1985. Assembly of asparagine-linked oligosaccharides. *Annu Rev Biochem.* 54:631–664.

Kranz C, Ng BG, Sun L, Sharma V, Eklund EA, Miura Y, Ungar D, Lupashin V, Winkel RD, Cipollo JF, et al. 2007. COG8 deficiency causes new congenital disorder of glycosylation type IIh. *Hum Mol Genet.* 16:731–741.

Linstedt AD, Mehta A, Suhan J, Reggio H, Hauri HP. 1997. Sequence and overexpression of GPP130/GIMPc: evidence for saturable pH-sensitive targeting of a type II early Golgi membrane protein. *Mol Biol Cell.* 8:1073–1087.

Livak KJ, Schmittgen TD. 2001. Analysis of relative gene expression data using real-time quantitative PCR and the $2^{-\Delta\Delta C_T}$ method. *Methods.* 25:402–408.

Lübbehusen J, Thiel C, Rind N, Ungar D, Prinsen BH, de Koning TJ, van Hasselt PM, Körner C. 2010. Fatal outcome due to deficiency of subunit 6 of the conserved oligomeric Golgi complex leading to a new type of congenital disorders of glycosylation. *Hum Mol Genet.* 19:3623–3633.

Ng BG, Kranz C, Hagebeuk EE, Duran M, Abeling NG, Wuyts B, Ungar D, Lupashin V, Hartdorff CM, Poll-The BT, et al. 2007. Molecular and clinical characterization of a Moroccan Cog7 deficient patient. *Mol Genet Metab.* 91:201–204.

Oka T, Ungar D, Hughson FM, Krieger M. 2004. The COG and COPI complexes interact to control the abundance of GEARs, a subset of Golgi integral membrane proteins. *Mol Biol Cell.* 15:2423–2435.

Oka T, Vasile E, Penman M, Novina CD, Dykxhoorn DM, Ungar D, Hughson FM, Krieger M. 2005. Genetic analysis of the subunit organization and function of the conserved oligomeric Golgi (COG) complex: Studies of COG5- and COG7-deficient mammalian cells. *J Biol Chem.* 280:32736–32745.

Paesold-Burda P, Maag C, Troxler H, Foulquier F, Kleinert P, Schnabel S, Baumgartner M, Hennet T. 2009. Deficiency in COG5 causes a moderate form of congenital disorders of glycosylation. *Hum Mol Genet.* 18:4350–4356.

Patterson GH, Hirschberg K, Polishchuk RS, Gerlich D, Phair RD, Lippincott-Schwartz J. 2008. Transport through the Golgi apparatus by rapid partitioning within a two-phase membrane system. *Cell.* 133:1055–1067.

Pelham HR, Rothman JE. 2000. The debate about transport in the Golgi—two sides of the same coin? *Cell.* 102:713–719.

Puri S, Bachert C, Fimmel CJ, Linstedt AD. 2002. Cycling of early Golgi proteins via the cell surface and endosomes upon lumenal pH disruption. *Traffic.* 3:641–653.

Ram RJ, Li B, Kaiser CA. 2002. Identification of Sec36p, Sec37p, and Sec38p: Components of yeast complex that contains Sec34p and Sec35p. *Mol Biol Cell.* 13:1484–1500.

Reynders E, Foulquier F, Leão Teles E, Quelhas D, Morelle W, Rabouille C, Annaert W, Matthijs G. 2009. Golgi function and dysfunction in the first COG4-deficient CDG type II patient. *Hum Mol Genet.* 18:3244–3256.

Shestakova A, Suvorova E, Pavliv O, Khaidakova G, Lupashin V. 2007. Interaction of the conserved oligomeric Golgi complex with t-SNARE Syntaxin5a/Sed5 enhances intra-Golgi SNARE complex stability. *J Cell Biol.* 179:1179–1192.

Shestakova A, Zolov S, Lupashin V. 2006. COG complex-mediated recycling of Golgi glycosyltransferases is essential for normal protein glycosylation. *Traffic.* 7:191–204.

Spaapen LJ, Bakker JA, van der Meer SB, Sijstermans HJ, Steet RA, Wevers RA, Jaeken J. 2005. Clinical and biochemical presentation of siblings with COG-7 deficiency, a lethal multiple O- and N-glycosylation disorder. *J Inherit Metab Dis.* 28:707–714.

Steet R, Kornfeld S. 2006. COG-7-deficient human fibroblasts exhibit altered recycling of Golgi proteins. *Mol Biol Cell.* 17:2312–2321.

Sun Y, Shestakova A, Hunt L, Sehgal S, Lupashin V, Storrie B. 2007. Rab6 regulates both ZW10/RINT-1 and conserved oligomeric Golgi complex-dependent Golgi trafficking and homeostasis. *Mol Biol Cell.* 18:4129–4142.

Suvorova ES, Duden R, Lupashin VV. 2002. The Sec34/Sec35p complex, a Ypt1p effector required for retrograde intra-Golgi trafficking, interacts with Golgi SNAREs and COPI vesicle coat proteins. *J Cell Biol.* 157:631–643.

Tai G, Lu L, Wang TL, Tang BL, Goud B, Johannes L, Hong W. 2004. Participation of the syntaxin 5/Ykt6/GS28/GS15 SNARE complex in transport from the early/recycling endosome to the trans-Golgi network. *Mol Biol Cell.* 15:4011–4022.

Ungar D, Oka T, Brittle EE, Vasile E, Lupashin VV, Chatterton JE, Heuser JE, Krieger M, Waters MG. 2002. Characterization of a mammalian Golgi-localized protein complex, COG, that is required for normal Golgi morphology and function. *J Cell Biol.* 157:405–415.

Ungar D, Oka T, Krieger M, Hughson FM. 2006. Retrograde transport on the COG railway. *Trends Cell Biol.* 16:113–120.

Van den Steen P, Rudd PM, Dwek RA, Opdenakker G. 1998. Concepts and principles of O-linked glycosylation. *Crit Rev Biochem Mol Biol*. 33:151–208.

Wu X, Steet RA, Bohorov O, Bakker J, Newell J, Krieger M, Spaapen L, Kornfeld S, Freeze HH. 2004. Mutation of the COG complex subunit gene COG7 causes a lethal congenital disorder. *Nat Med*. 10:518–523.

Xu Y, Martin S, James DE, Hong W. 2002. GS15 forms a SNARE complex with syntaxin 5, GS28, and Ykt6 and is implicated in traffic in the early cisternae of the Golgi apparatus. *Mol Biol Cell*. 13:3493–3507.

Zolov SN, Lupashin VV. 2005. Cog3p depletion blocks vesicle-mediated Golgi retrograde trafficking in HeLa cells. *J Cell Biol*. 168:747–759.